

Monitoring red tide with satellite imagery and numerical models: A case study in the Arabian Gulf

Jun Zhao ^{*}, Hosni Ghedira

Institute Center for Water and Environment (iWATER), Masdar Institute of Science and Technology, Masdar City, PO Box 54224, Abu Dhabi, United Arab Emirates

ARTICLE INFO

Keywords:

Red tide
Arabian Gulf
Remote sensing
Numerical model
Upwelling

ABSTRACT

A red tide event that occurred in August 2008 in the Arabian Gulf was monitored and assessed using satellite observations and numerical models. Satellite observations revealed the bloom extent and evolution from August 2008 to August 2009. Flow patterns of the bloom patch were confirmed by results from a HYCOM model. HYCOM data and satellite-derived sea surface temperature data further suggested that the bloom could have been initiated offshore and advected onshore by bottom Ekman layer. Analysis indicated that nutrient sources supporting the bloom included upwelling, *Trichodesmium*, and dust deposition while other potential sources of nutrient supply should also be considered. In order to monitor and detect red tide effectively and provide insights into its initiation and maintenance mechanisms, the integration of multiple platforms is required. The case study presented here demonstrated the benefit of combining satellite observations and numerical models for studying red tide outbreaks and dynamics.

© 2014 The Authors. Published by Elsevier Ltd. Open access under CC BY license.

1. Introduction

The Arabian Gulf is of paramount economic importance in the world. The tremendous oil resources and their maritime transports in the area have constantly drawn compelling attention.

The Arabian Gulf is a shallow, semi-enclosed marginal sea, which is connected to the Gulf of Oman through the Strait of Hormuz in the east (Fig. 1). Its mean depth is ~35 m, its length is ~990 km, and its maximal width is 370 km. The Arabian Gulf has asymmetric bathymetrical features along the main axis with a deeper zone off the Iranian coast and broad shallow shelf along the southern and western coasts from Kuwait to the United Arab Emirates (UAE). Additionally, the surrounding arid climate, in which evaporation surpasses the combination of precipitation and river runoff, results in hypersaline water mass production (Nezlin et al., 2010). These extreme conditions lead to an inverse estuarine circulation of cyclonic nature (Reynolds, 1993). The basin-scale circulation consists of two components. One current flows northwesterly from the Strait of Hormuz along the southern Iranian coast. The other one is a southeastern-flowing current in the southern Arabian Gulf (Reynolds, 1993). It flows out of the Arabian Gulf and spreads into the Gulf of Oman and the Arabian Sea at 200–300 m depth through the Strait of Hormuz (Prasad et al., 2001). The major rivers

that empty into the Arabian Gulf are located in the north and northwest with an average discharge rate of 36–1000 km³ year⁻¹ (Reynolds, 1993). The maximum river discharge was recorded in late spring-early summer (Nezlin et al., 2010). The precipitation over the Arabian Gulf area is very low at a rate of 0.07–0.1 m year⁻¹ (Marcella and Eltahir, 2008). Evaporation exceeds combined rainfall and freshwater discharge, which results in high salinity up to 44.3‰ (Jacob and Al-Muzaini, 1990). In addition to the high salinity, the Arabian Gulf is one of the warmest water bodies on earth with water temperature reaching 32 °C during the summer (ROPME, 1999). Other special characteristic of the Arabian Gulf region is its high aerosol concentration. Dust storms occur frequently in the gulf area, mainly in May–July, when dust deposition can amount to over 30 g m⁻² (Subba Rao and Al-Yamani, 1999).

Red tide, also known as harmful algal bloom, is caused by proliferation of a toxic or nuisance algae species and has been a pre-eminent topic of world-wide research communities for several decades (Cullen et al., 1997; Kahru et al., 2000; Stumpf et al., 2003; Ahn and Shanmugam, 2006; Gower et al., 2008; Zhao et al., 2008; Cannizzaro et al., 2008; Hu et al., 2011; Wang et al., 2011). Increasing frequency in red tide outbreaks has been reported around the world. It is of great concern due to not only their adverse effects on human health and marine organisms, but also their impacts on the economy of the affected areas. The recurrence of red tide depends on the species. Some species recur in the same area every year while others are episodic. The duration may differ from days to months.

The Arabian Gulf has been subject to red tide regularly with outbreaks recorded almost every year (Subba Rao and Al-Uamani,

* Corresponding author. Tel.: +971 28109125.

E-mail address: jzhao@masdar.ac.ae (J. Zhao).

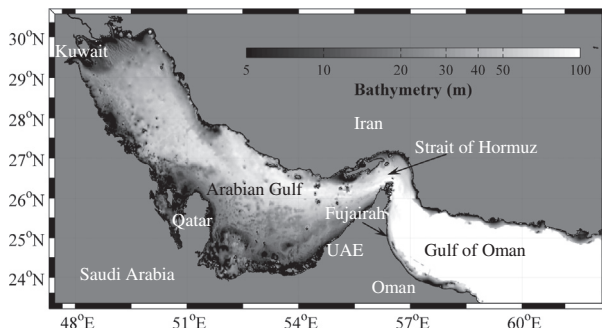


Fig. 1. Map of the study area. Overlaid are the bathymetry data with a spatial resolution of ~2 km from NOAA.

1998; Heil et al., 2001; Glibert et al., 2002; Moradi and Kabiri, 2012). A catastrophic red tide event happened in 2008 in the Arabian Gulf. Richlen et al. (2010) reported that the 2008 bloom was first observed on the east coast of the UAE in late August 2008 and dominated by *Cochlodinium polykriloides*. Although 38 types of taxa have been identified in the Arabian Gulf, *Cochlodinium polykriloides* was found for the first time in the region. Sale et al. (2011) demonstrated that the bloom patch dissipated in August 2009. According to Berkay (2011), the 2008 red tide event has affected more than 1200 km of coastline and has destroyed thousands of tons of fish and marine mammals. This disastrous event also did harm to local aquaculture (Richlen et al., 2010), coral reef community (Bauman et al., 2010), and fishery (Berkay, 2011). Additionally, red tide outbreaks could force the shutdown of desalination plants, which pose a major threat to the potable water supply (Berkay, 2011). Indeed, all Arabian Gulf countries rely on desalinated seawater for most of their potable water supply where 61% (17.1 M³ day⁻¹) of the global seawater desalination capacity is located along the Arabian Gulf coastlines (Lattemann et al., 2010).

For the reasons stated above, effective and timely observation of red tide is urgently required. Compared with conventional *in situ* ship surveys and buoy stations, which are time and cost consuming, satellite measurements have shown to be more effective in such applications thanks to their high spatial and temporal coverage over large scales. Furthermore, satellite measurements can cover regions unreachable for humans. For example, the 13-year of daily global imagery collected by the Sea-viewing Wide Field-of-view Sensor (SeaWiFS) at 1-km resolution was made available to the scientific community by NASA. To our knowledge, only two papers about the 2008 red tide event in the Arabian Gulf using satellite imagery have been published. Moradi and Kabiri (2012) used Moderate Resolution Imaging Spectroradiometer (MODIS) fluorescence data to detect the 2008 red tide with more focus on the Strait of Hormuz and the eastern region of the Arabian Gulf. Hamzei et al. (2012) have also investigated the 2008 red tide event using MODIS images and suggested that upwelling and sewage were the key nutrient sources that triggered the bloom in the Arabian Gulf and the Gulf of Oman. However, the 2008 red tide throughout the whole period has not been fully examined. Furthermore, the real causes of this bloom event is still unknown although Richlen et al. (2010) proposed that the 2008 bloom initiation may be related to monsoon-driven convective mixing. Meanwhile, the possible causes that might have led to the formation and lasting of the 12-month event have not been thoroughly studied yet.

Numerical model simulations offer an important and unique opportunity to improve our understanding of the mechanisms that regulate bloom initiation and evolution (He et al., 2008; Wang et al., 2011). Numerical models have been widely used for studies of algal bloom in other regions around the world (Olascoaga et al.,

2008; McGillicuddy et al., 2011). But to the best of our knowledge, there are no published papers on the use of numerical models to study algal blooms in the Arabian Gulf.

The main objectives of this paper are:

1. analyzing the formation and evolution of the 2008 red tide event in the Arabian Gulf using multisource satellite images and numerical models;
2. interpreting the initiation and sustaining mechanisms for the unusual long-lasting red tide event.

2. Data and method

In coastal waters, the accuracy of retrieving chlorophyll-a concentration based on the operational algorithms (O'Reilly et al., 1998) was significantly compromised due to the effects of other optically active components, i.e. suspended sediments and CDOM, which do not co-vary with chlorophyll-a (Mobley et al., 2004). Therefore, chlorophyll-a concentration alone is not sufficient to demonstrate bloom outbreaks. The feasibility of using ERGB images to differentiate bloom waters from other waters has been shown in previous studies (Hu et al., 2003, 2004; Zhao et al., 2013). In this work, satellite-derived chlorophyll-a concentration and ERGB images were used together as indicators of the 2008 bloom in the Arabian Gulf.

MODIS Aqua and Terra, SeaWiFS, and MERIS (Medium Resolution Imaging Spectrometer) data from August 2008 to September 2009 covering the study area (Fig. 1) were downloaded from NASA ocean color data archive. Only images with clear sky conditions were retained for further analysis. In total, 22 images were retained: 12 MODIS, 6 SeaWiFS and 4 MERIS. These images were processed using the most recent calibration and algorithms embedded in the SeaDAS package (version 6.4). Normalized water-leaving radiance (nL_w) at three wavelengths (i.e., 547 nm, 488 nm, and 443 nm for MODIS; 555 nm, 490 nm, and 443 nm for SeaWiFS; and 560 nm, 490 nm, and 443 nm for MERIS) was generated. Enhanced RGB (ERGB) images were composited using nL_w at the three wavelengths with 547 nm, 555 nm, and 560 nm as the red channel for discrete sensors. These ERGB images are very useful in differentiating different water types. Previous studies have suggested that brownish/reddish color is attributed to high concentrations of phytoplankton; the bright color is caused by sediment-rich waters and/or shallow bottom reflection; and the darkish color results from high concentration of phytoplankton and/or colored dissolved organic matter (CDOM) (Hu et al., 2003, 2004; Shanmugam et al., 2008; Simon and Shanmugam, 2012; Shanmugam, 2012; Zhao et al., 2013). Chlorophyll-a concentrations based on the default algorithms were also derived. Remote sensing reflectance (R_s) at 443, 469, 488, 531, 547, 555, 645, 667, and 678 nm, and sea surface temperature (SST) from MODIS were produced. All satellite images were then resampled to 1-km resolution for further analysis.

MODIS/Aqua derived 8-day composite SST images for 2008 and monthly mean aerosol optical thickness (AOT) at 869 nm images from 2002 to present with spatial resolution of 4 km were also acquired from NASA ocean color data achieve. The monthly climatology and anomaly of AOT were then calculated. The monthly anomaly was defined as the difference between the monthly mean and the corresponding monthly climatology.

HYbrid Coordinate Ocean Model (HYCOM) is a primitive equation ocean general circulation model (Bleck, 2002; Chassignet et al., 2009) that describes the effects of tide, wind, earth's rotation, and other factors on the ocean water flow. HYCOM derived surface current and sea surface height (SSH) were obtained from the HYCOM data server (www.hycom.org/dataserver) for chosen dates as shown in Fig. 3. HYCOM-derived ocean circulation data were

used to track red tide patches and help in detecting and forecasting of red tide outbreaks. They are also used to help in interpreting the initiation and propagation mechanisms of red tide events.

3. Results

Figs. 2 and 3 show representative chlorophyll-a and ERGB images, respectively, revealing the development and progression of the 2008 bloom event between August 2008 and August 2009. A high SeaWiFS chlorophyll-a patch was first detected on August 26 2008 in the coastal areas of the western Gulf of Oman. This patch can be clearly seen as dark feature in the corresponding ERGB image. The bloom patch remained in the area for a while. After late September, the original patch dispersed over a larger area and was separated into two parts. One moved eastward into the Gulf of Oman, and the other moved northward and entered the Arabian Gulf through the Strait of Hormuz. In October, the bloom patch was detected along the southern coast of Iran and along the western coast of UAE. Sample analysis indicated that cell counts amounted to $1.1\text{--}2.1 \times 10^7 \text{ cells L}^{-1}$ in October near Fujairah, UAE, and reached a maximum of $2.6 \times 10^7 \text{ cells L}^{-1}$ in October in the Strait of Hormuz (Richlen et al., 2010; Fatemi et al., 2012; Moradi and Kabiri, 2012). From early November till late November, the patch retreated a little bit and propagated into the Gulf of Oman. MERIS image observed on December 8 2008 showed that the bloom was advected into the Arabian Gulf again. The patch continued to disperse in the Arabian Gulf. In late December 2008, the patch extended over the southwestern coast of Iran, and north of Qatar and west of UAE, and remained through early February 2009. In some shallow areas, the bloom was hard to recognize due to shallow bottom or/and the presence of suspended sediments, as revealed by the bright feature in the ERGB images. Since

late February 2009, the bloom patch began to move toward the Strait of Hormuz and out into the Gulf of Oman. The satellite image collected on February 27 2009 showed that the bloom patch extended from the Strait of Hormuz to almost over the entire Gulf of Oman. This may be caused by the convergence of two bloom patches, one flowing out of the Strait of Hormuz from the Arabian Gulf and the other flowing northward from the Arabian Sea. This spatial distribution pattern remained till early April 2009. Since late April 2009, the bloom patch moved back into the Arabian Gulf again. From May to late June 2009, the bloom patch was mainly found along the western coast of UAE to the Strait of Hormuz, and in the eastern Gulf of Oman. From late July 2009 on, the bloom patch shrank gradually. In late August 2009, the bloom patch was gone. Although areas where the bloom patches were found in previous images had no valid satellite-derived chlorophyll-a data on August 30 2009, examination of all images one month after August 30 2009 indicated no suspicious features.

Fig. 4 shows the surface current vectors for dates corresponding to one day before those presented in Figs. 2 and 3. The movement patterns of bloom patches agreed well with numerical model results. These observations are in good agreement with previous similar studies where satellite observations were found to be a valuable source of information to track the dynamic of red tide blooms over large areas (Hu et al., 2011; Zhao et al., 2013).

4. Discussion

Being aware of the initiation process and spatial dynamic of red tide blooms can be profitable for biogeochemical forecasting models and provide evidence and operational guidelines for future decision-making mechanisms and emergency response actions. However, identifying the sources of nutrient supply to support

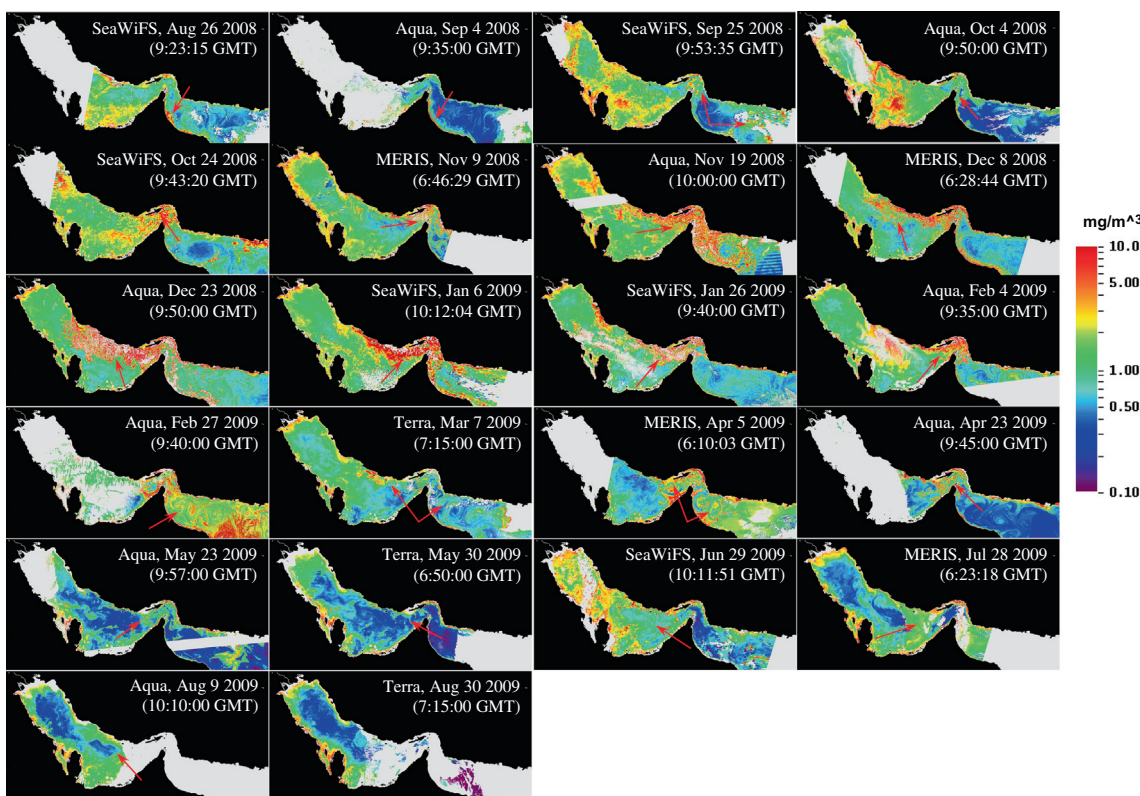


Fig. 2. Representative satellite-derived chlorophyll-a images showing the progression and development of the 2008 red tide event in the Arabian Gulf. Satellite data collection dates are also annotated. Images from SeaWiFS, MERIS, and MODIS Aqua and Terra, are used. Blank areas indicate no valid data due to cloud cover, heavy dust, or granule gap. The GMT time starts from mid-night. The red arrows show the positions of red tide. (For interpretation of the references to color in this figure legend, the reader is referred to the web version of this article.)

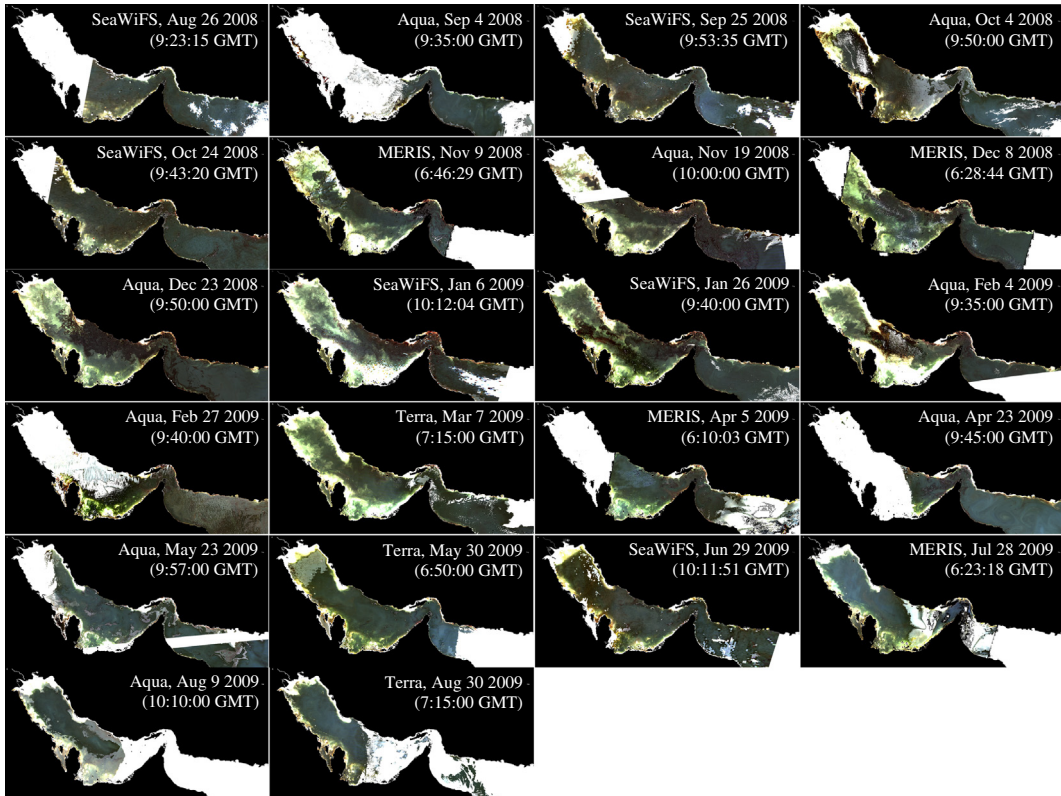


Fig. 3. Similar to Fig. 2, but for enhanced RGB (ERGB) images. ERGB images were composites with normalized water-leaving radiance (nL_w) at three bands, i.e. 547 nm, 488 nm, and 443 nm for MODIS; 555 nm, 490 nm, and 443 nm for SeaWiFS; and 560 nm, 490 nm, and 443 nm for MERIS. Blank areas indicate no valid data due to cloud cover, heavy dust, or granule gap. The GMT time starts from mid-night.

and maintain blooms is not straightforward and has always posed a challenge to researchers.

4.1. Initiation of the bloom

Since the outbreak of the 2008 bloom did not coincide with any record of large river discharges (Nezlin et al., 2010) and the freshwater inputs are low in the studied region, the bloom must have been initiated by other non-fluvial sources.

Richlen et al. (2010) suggested that the bloom may be related to physical forcing in the Arabian Sea, such as convective mixing. To investigate the potential role of physical forcing in triggering the 2008 bloom, surface ocean circulations from a HYCOM model were examined for the period preceding the first detected bloom patch observed on August 26 2008 (Fig. 2). The ocean circulation results indicated that the flow fields were upwelling favorable from August 7 onward. One example is shown in Fig. 5a. In the area where high SeaWiFS chlorophyll-a patch were found on August 26 2008, the surface current moved offshore and SSH was relatively low. Furthermore, the 8-day (August 23–30 2008) composite of MODIS/Aqua derived SST over the affected area was 0.5–1 °C lower than adjacent offshore waters (Fig. 5b). Therefore, it can be hypothesized that the bloom was initiated offshore and transported nearshore by bottom Ekman layer. This is similar to the observations made on the West Florida Shelf, where Weisberg et al. (2009) showed that the pathway of bloom to the nearshore was primarily via the bottom Ekman layer by an upwelling circulation.

4.2. Nutrient supplies for maintaining the bloom development

4.2.1. Upwelling

Fig. 6 shows an example of the existence of upwelling during the bloom period. The cold-core eddy was characterized by

anticlockwise spinning and relatively low SSH (Fig. 6a) and induced upwelling. MODIS derived SST on the same day (Fig. 6b) confirmed the occurrence of eddy-induced upwelling. Two patches of low temperature can be recognized north of UAE in the Strait of Hormuz and south of Iran in the Gulf of Oman, respectively. The anomalously low SST indicates that cold, nutrient-rich bottom waters was moved upward and subsequently provided nutrient supplies for phytoplankton growth. Cold-core eddies can also be identified in Fig. 4, e.g. south of Iran in the Arabian Gulf and in the eastern Gulf of Oman on September 24 2008. A La Niña episode occurred from late 2008 to early 2009. La Niña conditions have the effect of intensifying upwelling, which brings the pycnocline and nutricline up closer to the sea surface, more easily entrained into the upper euphotic zone (Linacre et al., 2010).

4.2.2. Dust deposition

AOT is an estimate of the particle loads in the air column, and has been used as an indicator of atmospheric turbidity (Volpe et al., 2009; Gallisai et al., 2012). Although high loads of atmospheric dust does not necessarily mean high deposition, strong positive correlations have been found between AOT and chlorophyll-a by Volpe et al. (2009). Additionally, these high dust levels affect significantly the chlorophyll-a estimates by increasing AOT estimates from satellite resulting in artificially high chlorophyll-a concentrations. Region-specific atmospheric correction algorithms calibrated and validated in the dusty environment of the Arabian Gulf would help to improve the accuracy of satellite-derived estimates. The contribution of dust-induced nutrients to the enhancement of marine productivity in the Arabian Gulf has been proposed by Hamza et al. (2011). Furthermore, Nezlin et al. (2010) showed that the atmospheric deposition is an important factor regulating phytoplankton growth in the Arabian Gulf. Fig. 7 presents the monthly anomaly of MODIS/Aqua derived AOT at 869 nm for

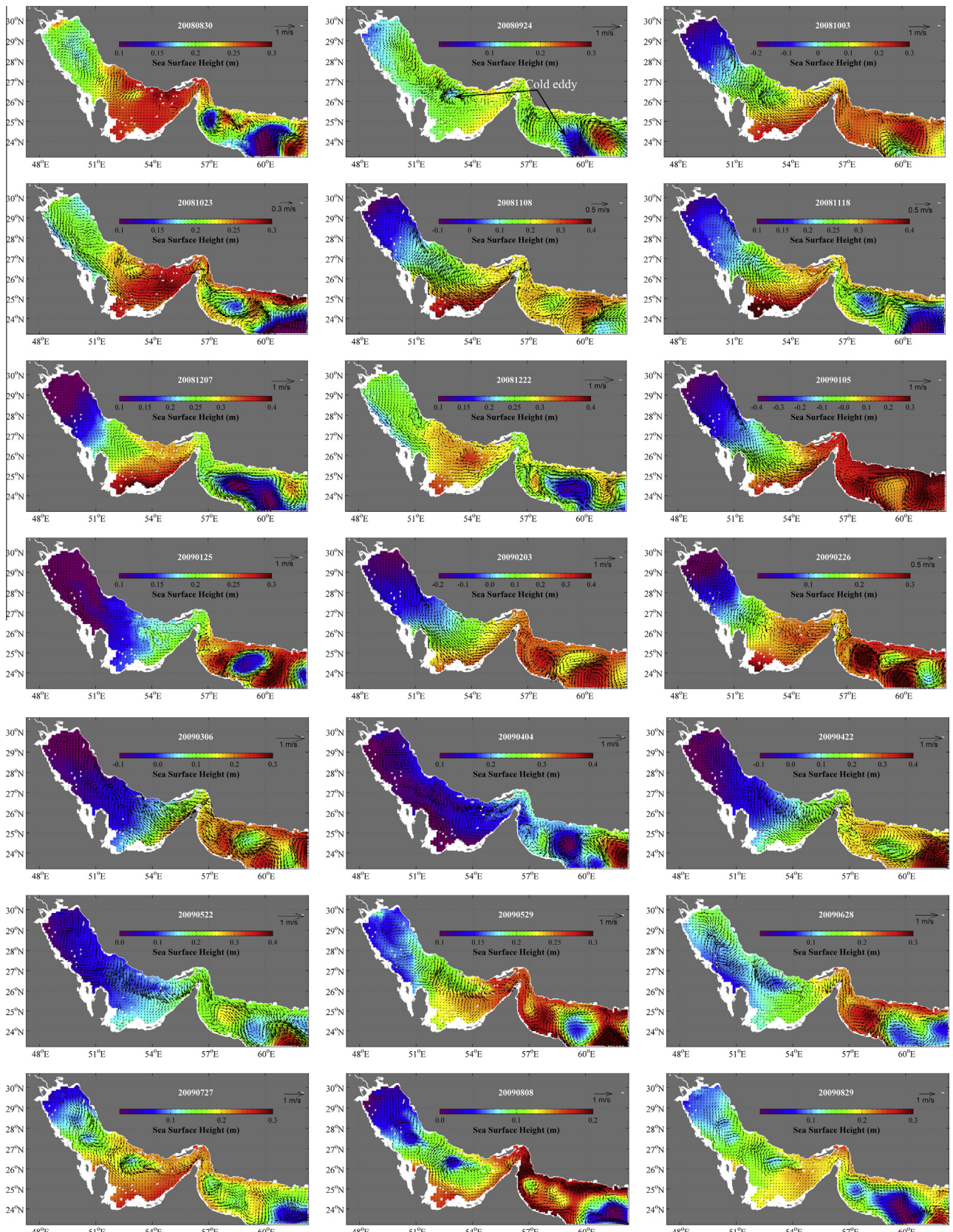


Fig. 4. Daily mean surface current vectors from a HYCOM model for dates corresponding to one day before those in Figs. 2 and 3. Data were downloaded from the HYCOM data server (www.hycom.org/dataserver). As indicated in the legend, some vector scales are different from others. Overlaid are sea surface height (SSH) data from the HYCOM model. Please note that the color scales of SSH for some panels are also different from others. Two cold eddies, characterized by counterclockwise rotation and lower SSH than surrounding waters, found on September 24 2008 are annotated as an example.(For interpretation of the references to colour in this figure legend, the reader is referred to the web version of this article.)

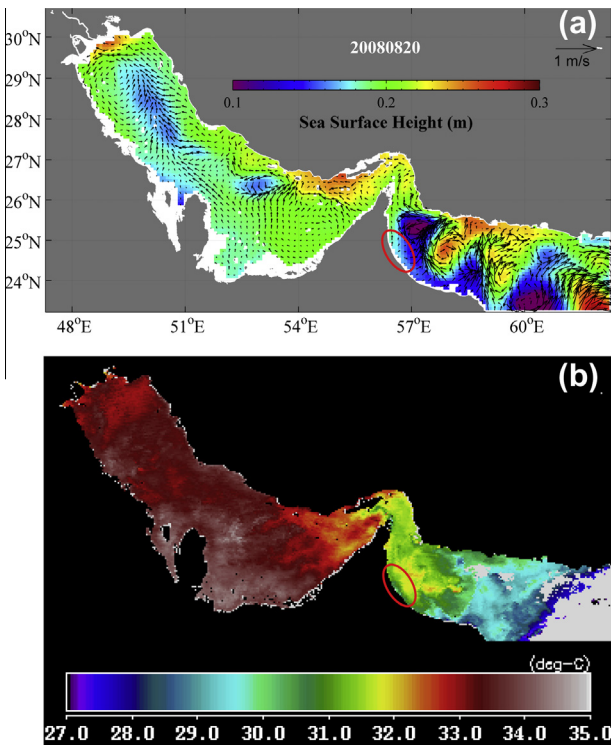


Fig. 5. (a) Daily mean surface current vectors from a HYCOM model for August 20 2008. HYCOM SSH data are overlaid. (b) 8-day composite of MODIS/Aqua derived sea surface temperature (SST) for August 23–30 2008. The resolution is 4 km. The red ellipses indicate the areas where a high chlorophyll-a patch was found on August 26 2008, as shown in Fig. 2. (For interpretation of the references to colour in this figure legend, the reader is referred to the web version of this article.)

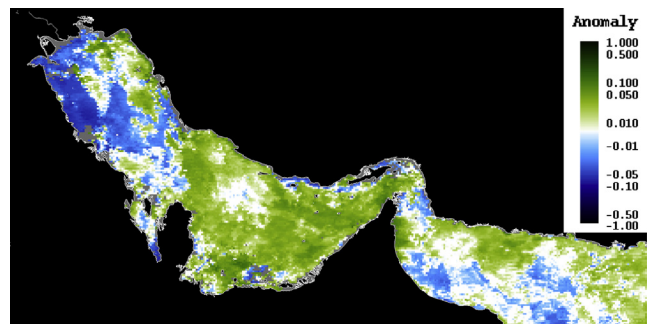


Fig. 7. Monthly anomaly of MODIS/Aqua derived aerosol optical thickness (AOT) at 869 nm for February 2009. The monthly anomaly was defined as the difference between the monthly mean and the monthly climatology. The monthly climatology was calculated for the period from 2002 to 2013.

February 2009. Positive anomalies were found in the middle and eastern Arabian Gulf, along the east coast of UAE, and in the north-eastern Gulf of Oman. Hence, dust deposition may have served as an important source of nutrient supply.

4.2.3. N-fixing *Trichodesmium*

Trichodesmium, a genus of cyanobacteria mainly found in tropical and subtropical marine waters, is commonly responsible for red tide outbreaks in the Arabian Gulf (Thangaraja et al., 2007; Miller and Wheeler, 2012). *Trichodesmium* can acclimate and grow at temperature ranging from 20 to 34 °C, and the maximum growth rate and maximum nitrogen fixing rate were found at the temperature range of 24–30 °C (Breitbarth et al., 2007). It can provide new nutrients for other blooms once initiated (Lenes et al., 2001; Walsh and Steidinger, 2001; Mulholland et al., 2004, 2006; Lenes and Heil, 2010).

With extensive *in situ* and MODIS data, Hu et al. (2010) showed that *Trichodesmium* presents unique spectral reflectance characteristics at 469, 488, 531, 547, 555 nm (i.e., high-low-high-low-high) due to specific optical properties of its unusual pigments and this spectral feature differentiate *Trichodesmium* blooms from other blooms. Fig. 8(a) and (b) display MODIS/Aqua derived ERGB and chlorophyll-a images for December 23 2008. The bloom patch showed high chlorophyll-a with brownish color in the ERGB image. Spectral analysis confirmed the presence of *Trichodesmium*, as indicated by the unique spectral curvature between 469 and 555 nm, i.e. high-low-high-low-high, shown in Fig. 8(c). The SST image presented in Fig. 8(d) shows that the temperature of the bloom patch vary in the range of 24–27 °C, which is also beneficial for growth of *Trichodesmium*, as aforementioned.

4.2.4. Other potential sources

The dominant species during the 2008 bloom period, dinoflagellate *Cochlodinium polykrikoides*, is mixotrophic (Jeong et al., 2004). It can respond directly to inorganic nutrients and dissolved organic substrates of anthropogenic origin and indirectly by consuming more abundant bacterial and algal prey that respond directly to elevated nutrients (Burkholder et al., 2008).

As suggested by Heil et al. (2001), aquaculture must be considered as additional source of nutrients that support bloom development. Industrial and sewage inputs contribute significantly. Inorganic nutrients and chronic oil pollution must also be taken into account, which enhances photosynthesis via reduction of pelagic and benthic grazers (Heil et al., 2001). Estuarine freshwater discharge from local rivers has also been considered as a source of nutrient supply for blooms, e.g. on the West Florida Shelf (Vargo et al., 2004; Brand and Compton, 2007; Stumpf et al., 2008).

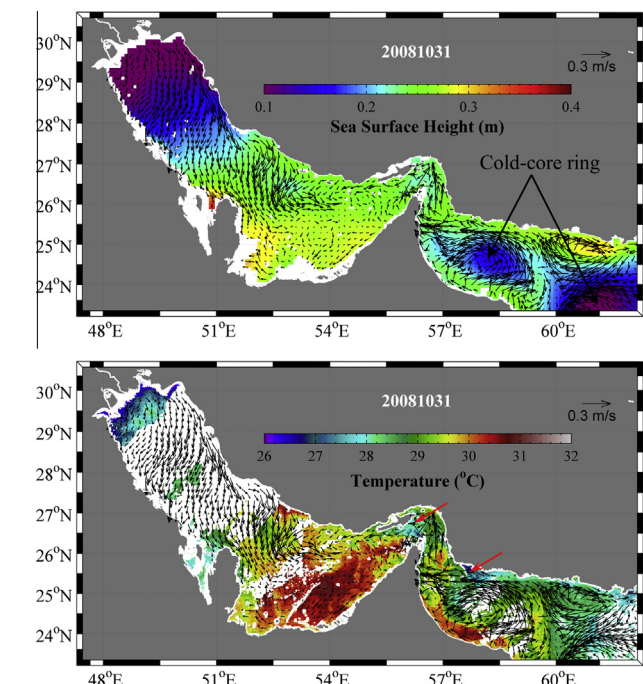


Fig. 6. HYCOM SSH (a) and MODIS/Aqua derived SST (b) for October 31 2008. Overlaid in both panels are daily mean surface current vectors. Two cold-core rings, as annotated by black arrows, can be apparently identified, which are characterized by counterclockwise rotation and lower SSH than surrounding waters. Two low temperature patches are annotated with red arrows, which indicate the occurrence of upwelling.

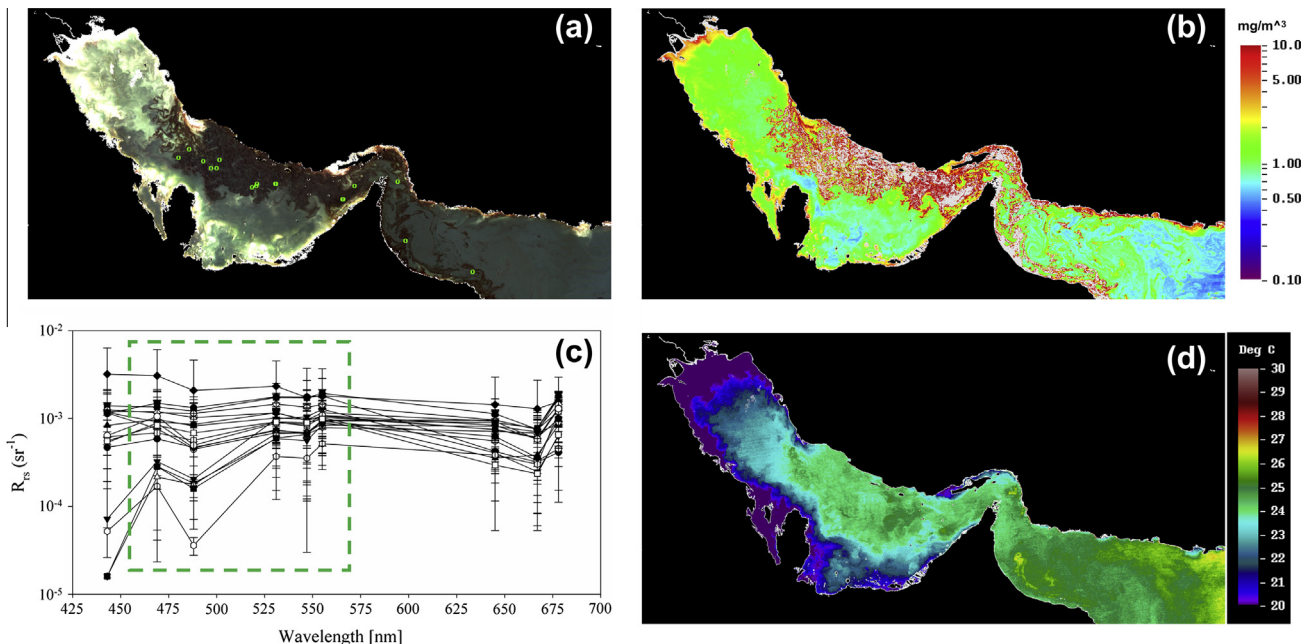


Fig. 8. MODIS/Aqua derived ERGB image (a), and chlorophyll-a concentration (b) for December 23 2008 (9:50 GMT). Panel (c) shows MODIS remote sensing reflectance (R_{rs}) spectra for the 18 stations annotated with green circles in (a). R_{rs} data were extracted from a window of 3×3 pixels centered at each station. The vertical bars show the standard deviations. The unique spectral features between 469 nm and 555 nm (high-low-high-low-high, as outlined by the green dashed box) indicate the presence of N-fixing *Trichodesmium*. Panel (d) shows the SST image collected by MODIS/Aqua on December 23 2008 (9:50 GMT). (For interpretation of the references to colour in this figure legend, the reader is referred to the web version of this article.)

However, estuarine nutrient flux alone is insufficient to support blooms (Walsh et al., 2006; Vargo et al., 2008). Submarine groundwater discharge (SGD) is a significant vector for solute transport between land and sea in arid climates (Ostrovsky, 2007). Hu et al. (2006) argued that submarine SGD could be another nutrient source for bloom development. SGD has also been reported in the Arabian Gulf (Ostrovsky, 2007). Walsh et al. (2009) showed that dead and decaying fish could sustain a bloom once the bloom was initiated.

4.3. Challenge in bloom observations

This paper showed the advantage of combining various observation techniques to monitor red tide evolution. The importance of such an integrated observation system has also been presented by English et al. (2009) and Weisberg et al. (2009). However, other challenges preventing us obtaining a complete picture still exist.

Limitations in satellite observations are well known, mainly caused by cloud cover and sun glint. As for the gulf region, high loads of atmospheric dust, which persist throughout the year, pose major challenges to effectively correct aerosol contributions to the satellite-measured reflectance. Continuous *in situ* measurements using autonomous platforms, such as autonomous underwater vehicle and autonomous profiling system, can fill the data gaps. Therefore, autonomous *in situ* measurements are strongly recommended for future activities.

Another challenge in monitoring red tide is that their initiation phase was very hard to capture. When the bloom was first detected by satellite imagery, the bloom has already formed. Based on coupled physical-biogeochemical modeling with appropriate configurations, forecasting models of potential blooms should be developed. Alternatively, resources permitting, routine deployment of autonomous platforms should be conducted to search for bottom layers of high biomass to prioritize the warnings of any potential outbreaks.

5. Conclusion

An extensive red tide event that occurred in 2008 in the Arabian Gulf was studied. Satellite imagery from several missions, including MODIS, MERIS, and SeaWiFS, was used to track the outbreak and evolution of the red tide event. The synoptic satellite observation captured the first signature of red tide in late August 2008 over the coastal areas of the western Gulf of Oman and revealed that the red tide event ended in late August 2009, lasting over a year. Numerical model simulation results demonstrated that the red tide was initiated offshore and transported onshore by bottom Ekman layer. Further analysis indicated that several factors contributed to the long-lasting red tide events, including upwelling, N-fixing *Trichodesmium*, dust deposition, river runoff, submarine groundwater discharge, aquaculture, industrial and sewage inputs, chronic oil pollution, and dead and decaying fish,

This case study shows an example of combining satellite observations and numerical ocean models to observe and interpret red tide events. The integrated observations not only showed the bloom's evolution in time, but also helped reveal the initiation and maintenance mechanisms. This study highlights the needs of integrating different platforms to establish a forecasting and monitoring system for adverse water quality events, such as red tide.

Acknowledgements

This investigative study is fully funded by Masdar Institute of Science and Technology, Abu Dhabi (UAE). We would like to thank NASA OBPG science team for providing satellite images and the National Ocean Partnership Program (NOPP) for providing SSH and ocean circulation data.

We also acknowledge the MODIS/SeaWiFS/MERIS mission scientists and principal investigators for the production of the data used in this research effort.

References

- Ahn, Y.-H., Shanmugam, P., 2006. Detecting the red tide algal blooms from satellite ocean color observations in optically complex Northeast-Asia coastal waters. *Remote Sensing of Environment* 103, 419–437.
- Bauman, A.G., Burt, J.A., Feary, D.A., Marquis, E., Usseglio, P., 2010. Tropical harmful algal blooms: an emerging threat to coral reef communities. *Marine Pollution Bulletin* 60 (11), 2117–2122.
- Berkay, A., 2011. Environmental approach and influence of red tide to desalination process in the Middle East region. *International Journal of Chemical and Environmental Engineering* 2 (3), 183–188.
- Beck, R., 2002. An oceanic general circulation model framed in hybrid isopycnic-Cartesian coordinates. *Ocean Modeling* 4, 55–58.
- Brand, L., Compton, A., 2007. Long-term increase in *Karenia brevis* abundance along the Southwest Florida Coast. *Harmful Algae* 6 (2), 232–252.
- Breitbarth, E., Oschlies, A., LaRoche, J., 2007. Physiological constraints on the global distribution of *Trichodesmium* – effect of temperature on diazotrophy. *Biogeosciences* 4, 53–61.
- Burkholder, J.M., Glibert, P.M., Skelton, H.M., 2008. Mixotrophy, a major mode of nutrition for harmful algal species in eutrophic waters. *Harmful Algae* 8, 77–93.
- Cannizzaro, J.P., Carder, K.L., Chen, F.R., Heil, C.A., Vargo, G.A., 2008. A novel technique for detection of the toxic dinoflagellate *Karenia brevis*, in the Gulf of Mexico from remotely sensed ocean color data. *Continental Shelf Research* 28, 137–158.
- Chassignet, E.P., Hurlbert, H.L., Metzger, E.J., Smedstad, O.M., Cummings, J.A., Wallcraft, A.J., Lozano, C., Tolman, H.L., Srinivasan, A., Hankin, S., Cornillon, P., Weisberg, R., Barth, A., He, R., Werner, F., Wilkin, J., 2009. US GODAE: Global Ocean Prediction With the Hybrid Coordinate Ocean Model (HYCOM). *Oceanography* 22, 48–59.
- Cullen, J.J., Ciotti, A.M., Davis, R.R., Lewis, M.R., 1997. Optical detection and assessment of algal blooms. *Limnology and Oceanography* 42 (5), 1223–1239.
- English, E., Hu, C., Lemke, C., Weisberg, R., Edwards, D., Lorenzoni, L., Gonzalez, G., Muller-Karger, F., 2009. Observing the 3-dimensional distribution of bio-optical properties of West Florida Shelf waters using gliders and autonomous platforms. *OCEANS 2009, MTS/IEEE Biloxi – Marine Technology for Our Future: Global and Local, Challenges, 26–29 October, 2009*, pp. 1–7.
- Fatemi, S.M.R., Nabavi, S.M.B., Vosoghi, G., Fallahi, M., Mohammadi, M., 2012. The relation between environmental parameters of Hormuzgan coastline in Persian Gulf and occurrence of the first harmful algal bloom of *Cochlodinium polykrikoides* (Gymnodiniaceae). *Iranian Journal of Fisheries Sciences* 11 (3), 475–489.
- Gallisai, R., Peters, F., Basart, S., Baldasano, J.M., 2012. Mediterranean basin-wide correlations between Saharan dust deposition and ocean chlorophyll concentration. *Biogeosciences Discussion* 9, 8611–8639. <http://dx.doi.org/10.5194/bgd-9-8611-2012>.
- Glibert, P.M., Landsberg, J.H., Evans, J.J., Al-Sarawl, M.A., Faraj, M., Al-Jarallah, M.A., Haywood, A., Ibrahim, S., Klesius, P., Powell, C., Shoemaker, C., 2002. A fish kill of massive proportion in Kuwait Bay, Arabian Gulf, 2001: the roles of bacterial disease, harmful algae, and eutrophication. *Harmful Algae* 1, 215–231.
- Gower, J.F.R., King, S.A., Goncalves, P., 2008. Global monitoring of plankton blooms using MERIS MCI. *International Journal of Remote Sensing* 29, 6209–6216.
- Hamza, W., Enan, M.R., Al-Hassini, H., Stuit, J.-B., de-Beer, D., 2011. Dust storms over the Arabian Gulf: a possible indicator of climate changes consequences. *Aquatic Ecosystem Health & Management* 14 (3), 260–268.
- Hamzei, S., Bidokhti, A.A., Mortazavi, M.S., Gheibi, A., 2012. Utilization of satellite imagers for monitoring harmful algal blooms at the Persian Gulf and Gulf of Oman. *2012 International Conference on Environmental, Biomedical and Biotechnology, IPCBEE, 41, IACSIT Press, Singapore*, pp. 171–174.
- He, R., McGillicuddy, Jr.D.J., Keafer, B.A., Anderson, D.M., 2008. Historic 2005 toxic bloom of *Alexandrium fundyense* in the western Gulf of Maine: 2. Coupled biophysical numerical modeling. *Journal of Geophysical Research* 113, C07040. <http://dx.doi.org/10.1029/2007JC004602>.
- Heil, C.A., Glibert, P.M., Al-Sarawl, M.A., Faraj, M., Behbehani, M., Husain, M., 2001. First record of a fishing-killing *Gymnodinium* sp bloom in Kuwait Bay, Arabian Sea: chronology and potential causes. *Marine Ecology Progress Series* 214, 15–23.
- Hu, C., Hackett, K.E., Callahan, M.K., Andréfouët, S., Wheaton, J.L., Porter, J.W., Muller-Karger, F.E., 2003. The 2002 ocean color anomaly in the Florida Bight: a cause of local coral reef decline? *Geophysical Research Letters*. <http://dx.doi.org/10.1029/2002GL016479>.
- Hu, C., Muller-Karger, F.E., Vargo, G.A., Neely, M.B., Johns, E., 2004. Linkages between coastal runoff and the Florida Keys ecosystem: a study of a dark plume event. *Geophysical Research Letters*. <http://dx.doi.org/10.1029/2004GL020382>.
- Hu, C., Müller-Karger, F.E., Swarzenski, P.W., 2006. Hurricanes, submarine groundwater discharge, and Florida's red tides. *Geophysical Research Letters* 33, L11601. <http://dx.doi.org/10.1029/2005GL025449>.
- Hu, C., Cannizzaro, J., Carder, K.L., Müller-Karger, F.E., Hardy, R., 2010. Remote detection of *Trichodesmium* blooms in optically complex coastal waters: examples with MODIS full-spectral data. *Remote Sensing of Environment* 114, 2048–2058.
- Hu, C., Cannizzaro, J., Carder, K.L., Lee, Z., Müller-Karger, F.E., Soto, I., 2011. Red tide detection in the eastern Gulf of Mexico using MODIS imagery. In: Morales, J., Stuart, V., Platt, T., Sathyendranath, S. (Eds.) (2011), *Handbook of Satellite Remote Sensing Image Interpretation: Applications for Marine Living Resources Conservation and Management*, EU PRESPO and IOCCG, Dartmouth, Canada, pp. 95–110.
- Jacob, P.G., Al-Muzaini, A., 1990. Marine plants of the Arabian Gulf: a literature review. *Kuwait Institute for Scientific Research, Safat, Kuwait (KISR Tech, Report No. 3426)*.
- Jeong, H.J., Yoo, Y.D., Kim, J.S., Kim, T.H., Kim, J.H., Kang, N.S., Yih, W., 2004. Mixotrophy in the phototrophic harmful alga *Cochlodinium polykrikoides* (Dinophycean): prey species, the effects of prey concentration, and grazing impact. *Journal of Eukaryotic Microbiology* 51 (5), 563–569.
- Kahru, M., Leppänen, J.M., Rud, O., Savchuk, O.P., 2000. Cyanobacteria blooms in the Gulf of Finland triggered by saltwater inflow into the Baltic Sea. *Marine Ecology Progress Series* 207, 13–18.
- Lattemann, S., Kennedy, M.D., Schippers, J.C., Gary, A., 2010. Global desalination situation. *Sustainability Science and Engineering* 2, 7–39.
- Lenes, J.M., Heil, C.A., 2010. A historical analysis of the potential nutrient supply from the N₂ fixing marine cyanobacterium *Trichodesmium* spp. to *Karenia brevis* in the eastern Gulf of Mexico. *Journal of Plankton Research* 32, 1421–1431.
- Lenes, J.M., Darrow, B.P., Cattrall, C., Heil, C.A., Callahan, M., Vargo, G.A., Byrne, R.H., Prospero, J.M., Bates, D.E., Fanning, K.A., 2001. Iron fertilization and the *Trichodesmium* response on the West Florida shelf. *Limnology and Oceanography* 46, 1261–1277.
- Linacre, L.P., Landry, M.R., Lara-Lara, J.R., Hernández-ayón, J.M., 2010. Picoplankton dynamics during contrasting seasonal oceanographic conditions at a coastal upwelling station off Northern Baja California, México. *Journal of Plankton Research* 32 (4), 539–557.
- Marcella, E.P., Eltahir, E.A.B., 2008. The hydroclimatology of Kuwait: explaining the variability of rainfall at seasonal and interannual time scales. *Journal of Hydrometeorology* 9 (5), 1095–1105.
- McGillicuddy Jr., D.J., Townsend, D.W., He, R., Keafer, B.A., Kleindinst, J.L., Li, Y., Manning, J.P., Mountain, D.G., Thomas, M.A., Anderson, D.M., 2011. Suppression of the 2010 *Alexandrium fundyense* bloom by changes in physical, biological, and chemical properties of the Gulf of Maine. *Limnology and Oceanography* 56 (6), 2411–2426.
- Miller, C.B., Wheeler, P.A., 2012. *Biological oceanography*, second ed., Wiley-Blackwell.
- Mobley, C.D., Stramski, D., Dissett, W.P., Boss, E., 2004. Optical modeling of ocean water: is the case 1 – case 2 classification still useful? *Oceanography* 17, 60–67.
- Moradi, M., Kabiri, K., 2012. Red tide detection in the Strait of Hormuz (east of the Persian Gulf) using MODIS fluorescence data. *International Journal of Remote Sensing* 33 (4), 1015–1028.
- Mulholland, M.R., Bronk, D.A., Capone, D.G., 2004. N₂ fixation and regeneration of NH₄⁺ and dissolved organic N by *Trichodesmium* IMS101. *Aquatic Microbial Ecology* 37, 85–94.
- Mulholland, M.R., Bernhardt, P.W., Heil, C.A., Bronk, D.A., O'Neil, J.M., 2006. Nitrogen fixation and release of fixed nitrogen by *Trichodesmium* spp. in the Gulf of Mexico. *Limnology and Oceanography* 51, 1762–1776.
- Nezlin, N.P., Polikarpov, I.G., Al-Yamani, F.Y., Rao, D.V.S., Ignatov, A.M., 2010. Satellite monitoring of climatic factors regulating phytoplankton variability in the Arabian (Persian) Gulf. *Journal of Marine Systems* 82, 47–60.
- Olascoaga, M.J., Beron-Vera, F.J., Brand, L.E., Koçak, H., 2008. Tracing the early development of harmful algal blooms on the West Florida Shelf with the aid of Lagrangian coherent structures. *Journal of Geophysical Research* 113, C12. <http://dx.doi.org/10.1029/2007JC004533>.
- O'Reilly, J.E., Maritorena, S., Mitchell, B.G., Siegel, D.A., Carder, K.L., Garver, S.A., Kahru, M., McClain, C., 1998. Ocean color chlorophyll algorithms for SeaWiFS. *Journal of Geophysical Research*, 103, C11, 24937–24953.
- Ostrovsky, V.N., 2007. Comparative analysis of groundwater formation in arid and super-arid deserts (with examples from Central Asia and northeastern Arabian Peninsula). *Hydrogeology* 15, 759–771.
- Prasad, T., G., Ikeda, M., Kumar, S.P., 2001. Seasonal spreading of the Persian Gulf Water mass in the Arabian Sea. *Journal of Geophysical Research-Oceans*, 106, C8, 17059–17071.
- Reynolds, M.R., 1993. Physical oceanography of the Gulf, Strait of Hormuz, and Gulf of Oman – results from the Mt. Mitchell expedition. *Marine Pollution Bulletin* 27, 35–39.
- Richlen, M.L., Morton, S.L., Jamali, E.A., Rajan, A., Anderson, D.M., 2010. The catastrophic 2008–2009 red tide in the Arabian gulf region, with observations on the identification and phylogeny of the fish-killing dinoflagellate *Cochlodinium polykrikoides*. *Harmful Algae* 9, 163–172.
- ROPME (Regional Organization for the Protection of the Marine Environment), 1999. Regional report of the state of the marine environment, regional organization for the protection of the marine environment, State of Kuwait, March 1999.
- Sale, P.F., Feary, D.A., Burt, J.A., Bauman, A.G., Cavalcante, G.H., Drouillard, K.G., Kjerfve, B., Marquis, E., Trick, C.C., Usseglio, P., Van Lavieren, H., 2011. The growing need for sustainable ecological management of marine communities of the Persian Gulf. *AMBIO*. <http://dx.doi.org/10.1007/s13280-010-0092-6>.
- Shanmugam, P., 2012. CAAS: an atmospheric correction algorithm for the remote sensing of complex waters. *Annales Geophysicae* 30, 203–220.
- Shanmugam, P., Ahn, Y.-H., Ram, P.S., 2008. SeaWiFS sensing of hazardous algal blooms and their underlying mechanisms in shelf-slope waters of the Northwest Pacific during summer. *Remote Sensing of Environment* 112, 3248–3270.

- Simon, A., Shanmugam, P., 2012. An algorithm for classification of algal blooms using MODIS-Aqua data in oceanic waters around India. *Advances in Remote Sensing* 1, 35–51.
- Stumpf, R.P., Culver, M.E., Tester, P.A., Tomlinson, M., Kirkpatrick, G.J., Pederson, B.A., Truby, E., Ransibrahmanakul, V., Soracco, M., 2003. Monitoring Karenia brevis blooms in the Gulf of Mexico using satellite ocean color imagery and other data. *Harmful Algae* 2 (2), 147–160.
- Stumpf, R.P., Litaker, R.W., Lanerolle, L., Tester, P.A., 2008. Hydrodynamic accumulation of Karenia off the west coast of Florida. *Continental Shelf Research* 28, 189–213.
- Subba Rao, D.V., Al-Uamani, F., 1998. Phytoplankton ecology in the water between Shatt Al-Arab and the Straits of Hormuz, Arabian Gulf: a review. *Plankton Biology Ecology* 45, 101–116.
- Subba Rao, D.V., Al-Yamani, F., 1999. Aeolian dust affects phytoplankton in the waters off Kuwait, the Arabian Gulf. *Naturwissenschaften* 86 (11), 525–529.
- Thangaraja, M., Al-Aisry, A., Al-Kharusi, L., 2007. Harmful algal blooms and their impacts in the middle and outer ROPME sea area. *International Journal of Oceans and Oceanography* 2 (1), 85–98.
- Vargo, G.A., Heil, C.A., Ault, D.N., Neely, M.B., Murasko, S., Havens, J., Lester, K.M., Dixon, L.K., Merkt, R., Walsh, J., Weisberg, R., Steidinger, K.A., 2004. Four Karenia brevis blooms: A comparative analysis, In: *Harmful Algae 2002*, Florida Fish and Wildlife Conservation Commission, Florida Institute of Oceanography and Intergovernmental Oceanographic Commission of UNESCO, pp. 14–16.
- Vargo, G.A., Heil, C.A., Fanning, K.A., Dixon, L.K., Neely, M.B., Lester, K., Ault, D., Murasko, S., Havens, J., Walsh, J., Bell, S., 2008. Nutrient availability in support of Karenia brevis blooms on the central West Florida Shelf: What keeps Karenia blooming? *Continental Shelf Research* 28, 73–98.
- Volpe, G., Banzon, V.F., Evans, R.H., Santoleri, R., Mariano, A.J., Sciarra, R., 2009. Satellite observations of the impact of dust in a low-nutrient, low-chlorophyll region: Fertilization or artifact? *Global Biogeochemical Cycles*, 23, GB3007, doi: 10.1029/2008GB003216.
- Walsh, J.J., Steidinger, K.A., 2001. Saharan dust and Florida red tides: the cyanophyte connection. *J. Geophys. Res.* 106, 11597–11612.
- Walsh, J.J., Jolliff, J.K., Darrow, B.P., Lenes, J.M., Milroy, S.P., Remsen, A., Dieterle, D.A., Carder, K.L., Chen, F.R., Vargo, G.A., Weisberg, R.H., Fanning, K.A., Müller-Karger, F.E., Shinn, E., Steidinger, K.A., Heil, C.A., Tomas, C.R., Prospero, J.S., Lee, T.N., Kirkpatrick, G.J., Whitley, T.E., Stockwell, D.A., Villareal, T.A., Jochens, A.E., Bontempi, P.S., 2006. Red tides in the Gulf of Mexico: where, when, and why? *Journal of Geophysical Research* 111, C11003. <http://dx.doi.org/10.1029/2004JC002813>.
- Walsh, J.J., Weisberg, R.H., Lenes, J.M., Chen, F.R., Dieterle, D.A., Zheng, L., Carder, K.L., Vargo, G.A., Havens, J.A., Peebles, E., Hollander, D.J., He, R., Heil, C.A., Mahmoudi, B., Landsberg, J.H., 2009. Isotopic evidence for dead fish maintenance of Florida red tides, with implications for coastal fisheries over both source regions of the West Florida Shelf and within downstream waters of the South Atlantic Bight. *Progress in Oceanography* 80, 51–73.
- Wang, G., Zhou, W., Cao, W., Yin, J., Yang, Y., Sun, Z., Zhang, Y., Zhao, J., 2011a. Variations of particulate organic carbon and its relationship with bio-optical properties during a phytoplankton bloom in the Pearl River estuary. *Marine Pollution Bulletin* 62 (9), 1939–1947.
- Wang, M., Liu, X., Shi, W., 2011. Hurricane-induced phytoplankton blooms: satellite observations and numerical model simulations. *Recent Hurricane Research – Climate, Dynamics, and Societal Impacts*. In: Prof. Anthony Lupo (Ed.), ISBN: 978978-953-307-238-8, InTech, Available from: <<http://www.intechopen.com/books/recent-hurricane-research-climate-dynamics-and-societal-impacts/hurricane-induced-phytoplankton-blooms-satellite-observations-and-numerical-model-simulations>>.
- Weisberg, R.H., Bartha, A., Alvera-Azcáratea, A., Zheng, L., 2009. A coordinated coastal ocean observing and modeling system for the West Florida Continental Shelf. *Harmful Algae* 8, 585–597.
- Zhao, J., Cao, W., Yang, Y., Wang, G., Zhou, W., Sun, Z., 2008. Measuring natural phytoplankton fluorescence and biomass a case study of algal bloom in the Pearl River estuary. *Marine Pollution Bulletin* 10, 1795–1801.
- Zhao, J., Hu, C., Lapointe, B., Melo, N., John, E.M., Smith, R.H., 2013. Satellite-observed black water events off southwest Florida: implications for coral reef health in the Florida Keys National Marine Sanctuary. *Remote Sensing* 5, 415–431. <http://dx.doi.org/10.3390/rs5010415>.